

# Resonance Occupation in the Kuiper Belt: Case Examples of the 5:2 and Trojan Resonances

E. I. Chiang<sup>1</sup>, A. B. Jordan<sup>1</sup>, R. L. Millis<sup>2</sup>, M. W. Buie<sup>2</sup>, L. H. Wasserman<sup>2</sup>,  
J. L. Elliot<sup>2,3,4</sup>, S. D. Kern<sup>3</sup>, D. E. Trilling<sup>5</sup>, K. J. Meech<sup>6</sup>, & R. M. Wagner<sup>7</sup>

echiang@astron.berkeley.edu

## ABSTRACT

As part of our ongoing Deep Ecliptic Survey (DES) of the Kuiper belt, we report on the occupation of the 1:1 (Trojan), 4:3, 3:2, 7:4, 2:1, and 5:2 Neptunian mean-motion resonances (MMRs). The previously unrecognized occupation of the 1:1 and 5:2 MMRs is not easily understood within the standard model of resonance sweeping by a migratory Neptune over an initially dynamically cold belt. Among all resonant Kuiper belt objects (KBOs), the three observed members of the 5:2 MMR discovered by DES possess the largest semi-major axes ( $a \approx 55.4$  AU), the highest eccentricities ( $e \approx 0.4$ ), and substantial orbital inclinations ( $i \approx 10^\circ$ ). Objects (38084) 1999HB<sub>12</sub> and possibly 2001KC<sub>77</sub> can librate with modest amplitudes of  $\sim 90^\circ$  within the 5:2 MMR for at least 1 Gyr. Their trajectories cannot be explained by close encounters with Neptune alone, given the latter's current orbit. The dynamically hot orbits of such 5:2 resonant KBOs, unlike hot orbits of previously known resonant KBOs, may imply that these objects were pre-heated to large inclination and large eccentricity prior to

---

<sup>1</sup>Center for Integrative Planetary Sciences, Astronomy Department, University of California at Berkeley, Berkeley, CA 94720

<sup>2</sup>Lowell Observatory, 1400 West Mars Hill Road, Flagstaff, AZ 86001

<sup>3</sup>Department of Earth, Atmospheric, and Planetary Sciences, Massachusetts Institute of Technology, 77 Massachusetts Avenue, Cambridge, MA 02139

<sup>4</sup>Department of Physics, Massachusetts Institute of Technology, 77 Massachusetts Avenue, Cambridge, MA 02139

<sup>5</sup>University of Pennsylvania, Department of Physics and Astronomy, David Rittenhouse Laboratory, 209 S. 33rd St., Philadelphia, PA 19104

<sup>6</sup>Institute for Astronomy, 2680 Woodlawn Drive, Honolulu, HI 96822

<sup>7</sup>Large Binocular Telescope Observatory, University of Arizona, Tucson, AZ 85721

resonance capture by a migratory Neptune. Our first discovered Neptunian Trojan, 2001QR<sub>322</sub>, may not owe its existence to Neptune’s migration at all. The trajectory of 2001QR<sub>322</sub> is remarkably stable; the object can undergo tadpole-type libration about Neptune’s leading Lagrange (L4) point for at least 1 Gyr with a libration amplitude of 24°. Trojan capture probably occurred while Neptune accreted the bulk of its mass. For an assumed albedo of 12–4%, our Trojan is  $\sim$ 130–230 km in diameter. Model-dependent estimates place the total number of Neptune Trojans resembling 2001QR<sub>322</sub> at  $\sim$ 20–60. Their existence might rule out violent orbital histories for Neptune.

*Subject headings:* Kuiper belt — comets: general — minor planets, asteroids — celestial mechanics

## 1. INTRODUCTION

A fraction of Kuiper belt objects (KBOs) occupy low-order, exterior mean-motion resonances (MMR) established by Neptune. Among the most well-known resonant KBOs are the Plutinos which occupy the 3:2 MMR (Jewitt & Luu 2000). Plutinos have substantial orbital eccentricities,  $0.1 \lesssim e \lesssim 0.3$ , an observation commonly interpreted to imply that Neptune migrated outwards by several AU early in the history of the solar system (Malhotra 1995). The standard model of resonant capture and adiabatic excitation by a migratory Neptune predicts the 2:1, 5:3, 7:4, 3:2, and 4:3 MMRs to be occupied by high eccentricity objects (Malhotra et al. 2000; Chiang & Jordan 2002, hereafter CJ). Occupation of the 4:3 MMR and possibly of the 2:1 MMR has been reported by Nesvorný & Roig (2001). Implications of Neptune’s migration for the Plutinos and the “Twotinos” (2:1 resonant KBOs) are explored in detail by CJ.

We report here, as part of the ongoing survey of the Kuiper Belt by the Deep Ecliptic Survey Team (Millis et al. 2002; Elliot et al. 2003), the previously unrecognized occupation of the 5:2 and 1:1 (Trojan) Neptunian resonances. The three observed members of the 5:2 MMR stand out among all resonant KBOs in having the largest semi-major axes ( $a \approx 55.4$  AU), the highest eccentricities ( $e \approx 0.4$ ), and substantial orbital inclinations ( $i \approx 10^\circ$ ). We will see that their dynamically hot orbits cannot be interpreted as initially dynamically cold orbits that were modified purely by resonance sweeping. Their existence points to another dynamical excitation mechanism that likely operated prior to Neptune’s migration.

Our discovery of the first Neptunian Trojan librating about the leading Lagrange (L4) point of Neptune vindicates theoretical suggestions as to the long-term orbital stability of

Neptunian Trojans (Holman & Wisdom 1993; Holman 1995; Gomes 1998; Nesvorny & Dones 2002). For example, Nesvorny & Dones (2002) find that about 50% of their hypothesized Neptunian Trojan population survives for 4 Gyr despite perturbations exerted by the other giant planets. The stability of Neptune’s Trojan population contrasts with the instability characterizing Saturnian and Uranian Trojans on  $10^8$  yr timescales (Nesvorny & Dones 2002; Gomes 1998).

In §2, we outline our procedure for identifying resonant KBOs in the face of observational uncertainties in their orbits, and describe the dynamical characteristics of our 5:2 and 1:1 resonant KBOs. Results of Gyr-long orbit integrations of our Trojan are presented at the end of this section. In §3, we briefly assess the plausibility of some theoretical scenarios that attempt to explain the observed pattern of resonance occupation. We consider models in which Neptune either sweeps objects into its resonances by virtue of its migration, or populates the resonances by direct, violent gravitational scattering. A summary of our results, interpreted in the context of theoretical models, is provided in §4.

## 2. Observed Resonance Membership

### 2.1. Classification Procedure

An object occupies a MMR if the resonant argument associated with that MMR librates. For the 5:2,  $e^3$  (third degree in the eccentricity of the KBO) Neptunian MMR, the argument is  $\phi_{5:2} = 5\lambda - 2\lambda_N - 3\tilde{\omega}$ , where  $\lambda$  and  $\tilde{\omega}$  are the mean longitude and longitude of pericenter of the object, respectively, and  $\lambda_N$  is the mean longitude of Neptune. For the 1:1,  $e^0$  Neptunian MMR, the argument equals  $\phi_{1:1} = \lambda - \lambda_N$ .

Testing for libration is a straightforward matter of integrating forward (or backward) the trajectory of an object in the gravitational fields of the Sun and the planets. A secure identification of a resonant KBO is made difficult by often substantial uncertainties in the initial position and velocity of the object, i.e., uncertainties in the osculating Keplerian ellipse fitted to astrometric observations. Bernstein & Khushalani (2000) derive a formalism for estimating these errors that is tailored for short arc astrometric observations. Our Deep Ecliptic Survey (DES; Millis et al. 2002; Elliot et al. 2003) utilizes their formalism.

Figures 1 and 2 depict the  $1\sigma$  and  $2\sigma$  confidence regions projected onto the  $a$ – $e$  plane of our three 5:2 resonant candidates and our one 1:1 resonant candidate. Uncertainties in  $a$  and  $e$  for these particular objects are small, of order 0.1%, thanks to the relatively extended, 1+ year-long arcs of astrometry available for these KBOs. All elements reported in this paper are osculating, heliocentric elements referred to the J2000 ecliptic plane, evaluated at epoch

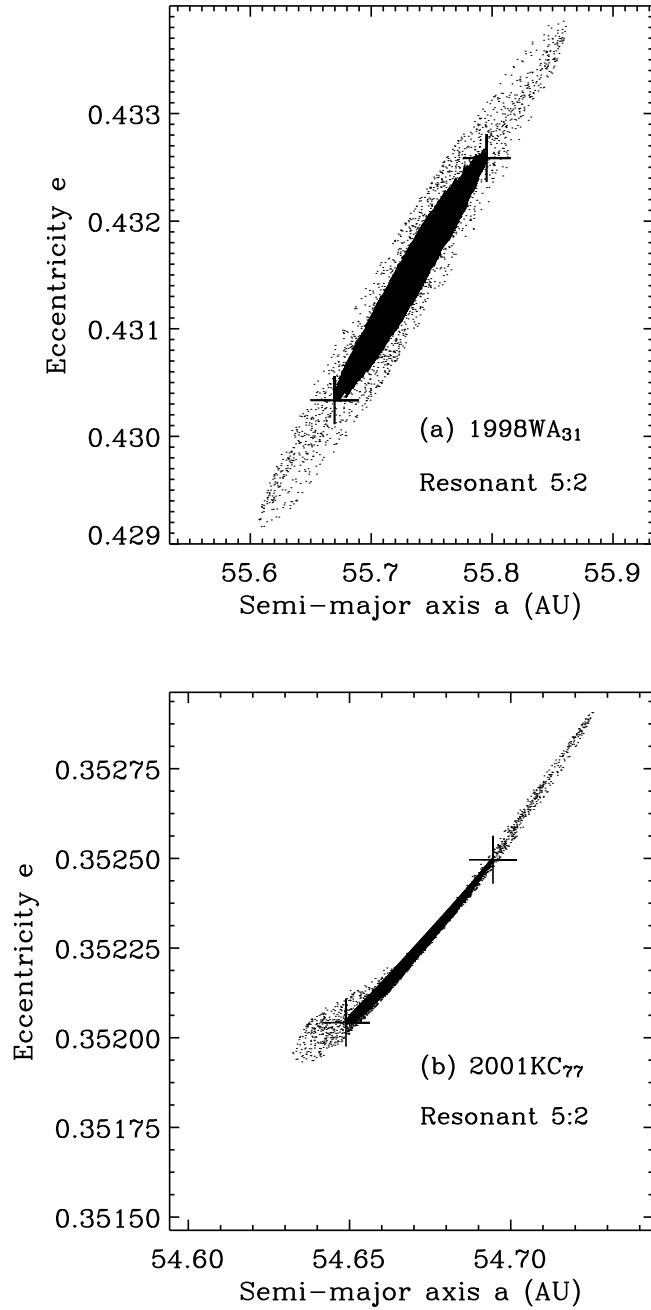


Fig. 1.— Projections onto the  $a$ - $e$  plane of the  $1\sigma$  and  $2\sigma$  confidence surfaces in the 6-dimensional phase space of possible osculating orbits for 5:2 resonant KBOs (a) 1998WA<sub>31</sub>, and (b) 2001KC<sub>77</sub>. Solid black areas correspond to  $1\sigma$  confidence regions, while speckled areas correspond to  $2\sigma$  confidence regions. The exact center of each plot corresponds to orbit solution 1, while crosses denote orbit solutions 2 and 3.

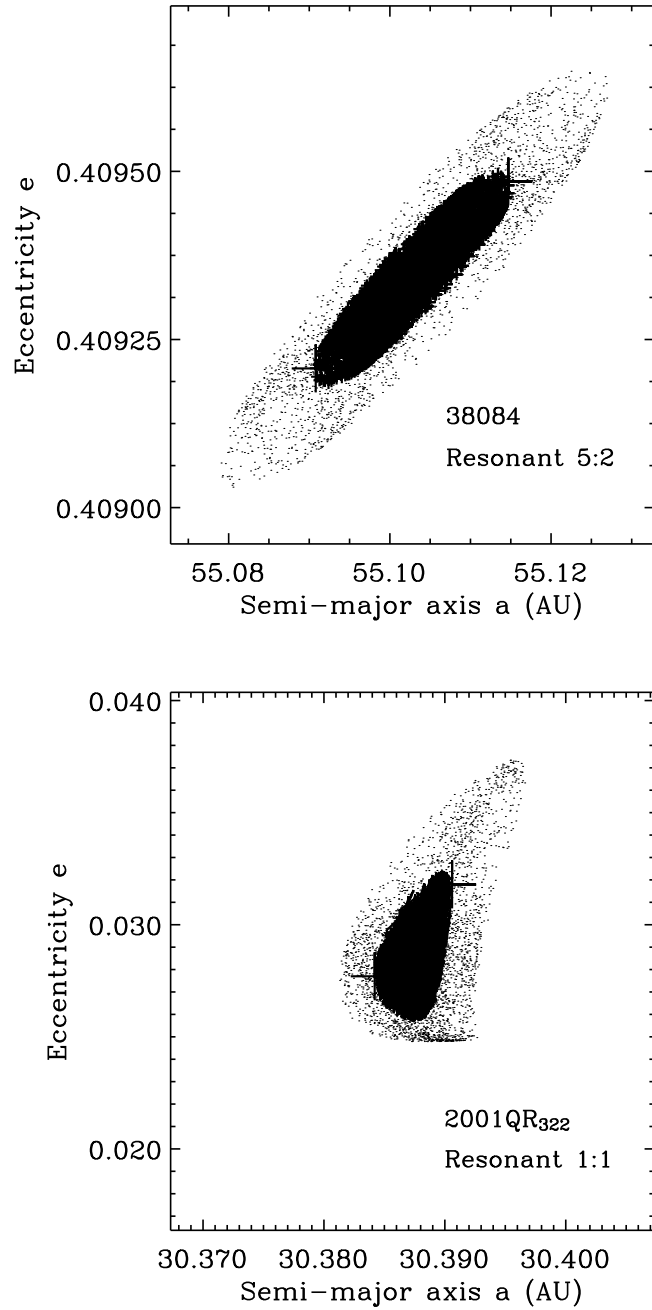


Fig. 2.— Projections onto the  $a$ - $e$  plane of the  $1\sigma$  and  $2\sigma$  confidence surfaces in the 6-dimensional phase space of possible osculating orbits for (a) (38084) 1999HB<sub>12</sub>, a 5:2 resonant KBO, and (b) 2001QR<sub>322</sub>, a 1:1 resonant KBO. Solid black areas correspond to  $1\sigma$  confidence regions, while speckled areas correspond to  $2\sigma$  confidence regions. The exact center of each plot corresponds to orbit solution 1, while crosses denote orbit solutions 2 and 3.

2451545.0 JD.

Surveying for libration in the 6-dimensional confidence volume of possible initial orbits for each of hundreds of KBOs discovered by our Deep Ecliptic Survey is daunting. We proceed with a more limited agenda; in the 6-D error volume appropriate to a given KBO, we integrate, in addition to the nominal best-fit (initial) osculating orbit, two other solutions that lie on the  $1\sigma$  confidence surface and that have the greatest and least semi-major axes. We refer to these sets of initial conditions as orbit solutions 1, 2, and 3, respectively. The other 5 orbital elements are adjusted according to their correlation with semi-major axis on the  $1\sigma$  confidence surface. We favor exploring the widest excursion in semi-major axis because that is the parameter that most influences resonance membership. The next most important parameter is eccentricity; however, as is evident in Figures 1 and 2, deviations in  $a$  and  $e$  are often strongly correlated, so that exploring the greatest deviation in  $a$  often implies that we are also exploring the greatest deviation in  $e$ . Our choice of focussing on variations in  $a$  is further supported by the fact that fractional errors in  $a$  (and  $e$ ) are slower to converge to zero than errors in  $i$  (Millis et al. 2002).

We numerically integrate three sets of initial conditions for each of 204 KBOs discovered by the DES collaboration as of April 9 2002 and given preliminary designations by the Minor Planet Center. We employ the regularized, mixed variable symplectic integrator, `swift_rmvs3`, developed by Levison & Duncan (1994) and based on the N-body map of Wisdom & Holman (1991). We include the influence of the four giant planets, treat each KBO as a massless test particle, and integrate trajectories forward for  $3 \times 10^6$  yr using a timestep of 50 days, starting at Julian date 2451545.0. Initial positions and velocities for all objects are computed using the formalism of Bernstein & Khushalani (2000) in the case of short-arc orbits, and from E. Bowell’s database in the case of long-arc orbits (see Millis et al. 2002). The relative energy error over the integration is bounded to less than  $10^{-7}$ . One hundred and seven different resonant arguments are examined for libration. Full details of our procedure are provided in Elliot et al. (2003).

Some results of this procedure are showcased in Figure 3, which contains only a small subset of the data to be released by Elliot et al. (2003). Only “secure” resonant objects are displayed; by “secure,” we mean that the  $1\sigma$  fractional uncertainties in semi-major axis are less than 10% and that all three sets of initial conditions give consistent orbit classifications over 3 Myr. A resonant object is one for which all three orbit solutions yield libration of one or more of the same resonant arguments; non-resonant objects exhibit no libration of any resonant argument among the three solutions. The locations of the points in Figure 3 correspond to the semi-major axes, eccentricities, and inclinations at the start of the integration. Error contours are much smaller than the sizes of the symbols in most

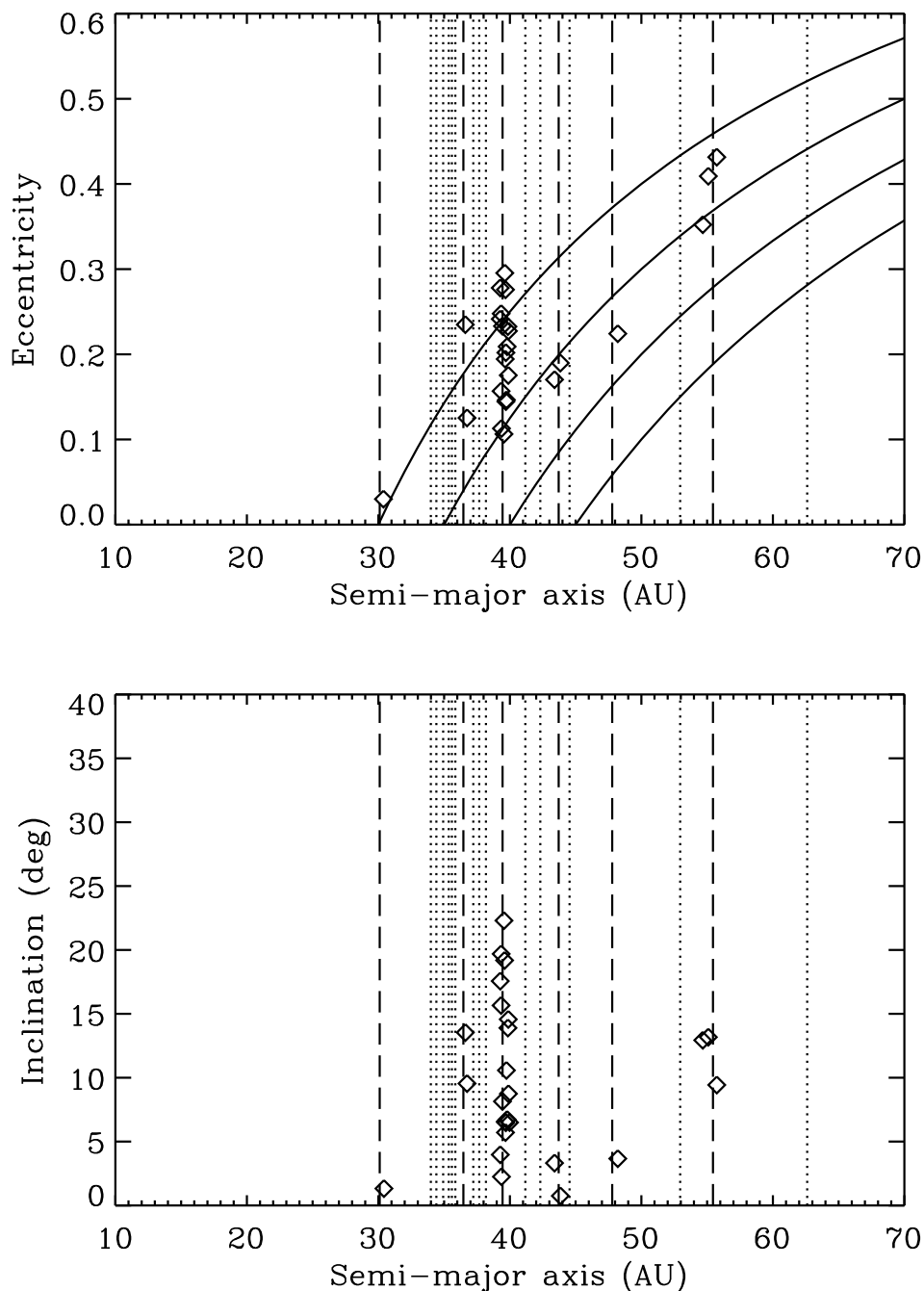


Fig. 3.— Eccentricities, inclinations, and semi-major axes of resonant KBOs found in the Deep Ecliptic Survey. For all displayed objects, fractional  $1\sigma$  uncertainties in semi-major axis range from 0.003% to 3.5%, and orbit solutions 1, 2, and 3 yield consistent orbital classifications. Open diamonds represent resonant objects only; non-resonant objects will be presented by Elliot et al. (2003). Vertical lines indicate locations of nominal resonance with Neptune; dotted lines indicate uninhabited resonances, while dashed lines indicate inhabited resonances. Solid curves correspond to perihelion distances of 30, 35, 40, and 45 AU. Resonances with secure members include, in order of increasing distance from Neptune, the 1:1, 4:3, 3:2, 7:4, 2:1, and 5:2 MMRs.

cases. Dashed lines delineate the locations of nominal resonance with Neptune. In addition to confirmed librators in the 4:3, 3:2, 7:4, and 2:1 resonances, the 1:1 and 5:2 resonances contain one and three members, respectively.

Figure 3 displays only objects discovered by the DES collaboration. Other groups have reported occupation of the 3:2, 4:3, and 2:1 resonances. For example, Nesvorný & Roig (2001) have reported KBOs occupying the 4:3 MMR and possibly the 2:1 MMR. When we integrate the trajectories of non-DES objects, we confirm the results of Nesvorný & Roig (2001) that 1995DA<sub>2</sub> inhabits the 4:3 MMR and that (20161) 1996TR<sub>66</sub> and 1997SZ<sub>10</sub> inhabit the 2:1 MMR. The names of resonant objects discovered by the DES team and by non-DES teams are contained in Table 2.

Whereas the 4:3, 3:2, 7:4, and 2:1 are predicted by the standard migration model for Neptune to be substantially populated (see Figures 3 and 4 of CJ), the 5:2 and 1:1 resonances are not. We focus our attention now on the newly discovered members of the 5:2 and 1:1 MMRs, to investigate the constraints they place on the dynamical history of the Kuiper belt.

## 2.2. Observed Members of the 5:2 MMR

Evolutions of the resonant argument,  $\phi_{5:2}$ , for objects 1998WA<sub>31</sub>, (38084) 1999HB<sub>12</sub>, and 2001KC<sub>77</sub> are displayed in Figure 4. The integrations shown begin with nominal best-fit initial conditions; the other two sets of initial conditions yield nearly identical results. The resonant argument,  $\phi_{5:2}$ , librates in the manner shown in Figure 4 for the entire duration of the integration, 3 Myr. The libration centers are  $\langle \phi_{5:2} \rangle = 180^\circ$ , the amplitudes are  $\Delta\phi_{5:2} \equiv \max \phi_{5:2} - \langle \phi_{5:2} \rangle \approx 90^\circ\text{--}140^\circ$ , and the libration periods are  $T_l \approx 2 \times 10^4$  yr. The libration period increases with decreasing libration amplitude, unlike the case for the conventional pendulum model for a resonance.

For each object, we further explore error space by integrating 8 additional sets of initial conditions that lie on the  $2\sigma$ ,  $3\sigma$ ,  $4\sigma$ , and  $5\sigma$  confidence surfaces and that are characterized by semi-major axes that deviate most from the best-fit semi-major axis in positive and negative senses. Objects (38084) 1999HB<sub>12</sub> and 2001KC<sub>77</sub> remain in the 5:2  $e^3$  resonance in all cases for 3 Myr. We conclude that our identifications of (38084) 1999HB<sub>12</sub> and 2001KC<sub>77</sub> as current 5:2 librators are particularly secure. Object 1998WA<sub>31</sub> fails to librate in the 5:2 resonance when its initial semi-major axis is less than the nominal value by  $2\sigma$  or more, i.e., when  $a$  is less than the nominal value by more than 0.13 AU. However, other sets of initial conditions for which  $a$  is greater than the nominal value yield libration even at the  $5\sigma$  level for 1998WA<sub>31</sub>. Our identification of 1998WA<sub>31</sub> as a current member of the resonance



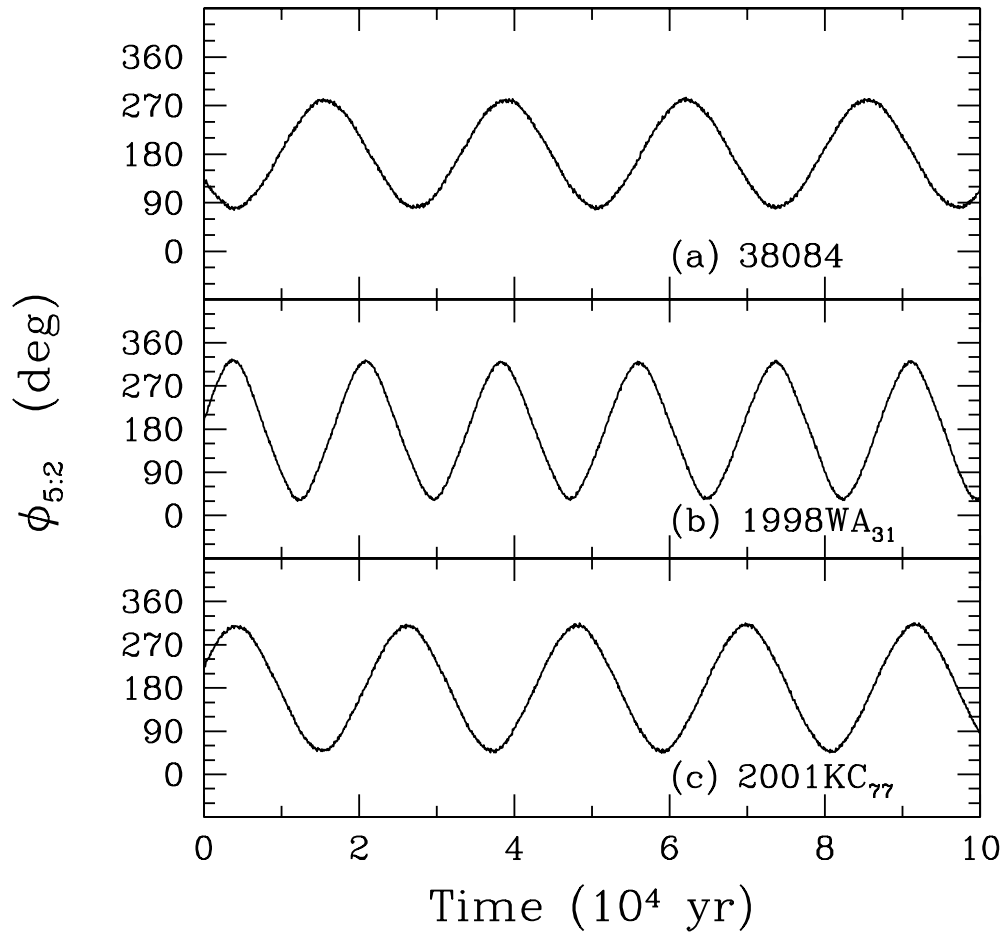


Fig. 4.— Libration of the resonant argument,  $\phi_{5:2}$ , for our observed members of the 5:2 resonance. Integrations begin with nominal best-fit initial conditions (orbit solution 1).

is therefore less firm than for the others, but not alarmingly so.

What is the long-term evolution of these objects? We have integrated orbit solutions 1, 2, and 3 for all three objects forward by 1 Gyr. For (38084) 1999HB<sub>12</sub>, all 3 orbit solutions yield libration in the 5:2 resonance for the full duration of the integration. The same is true for orbit solution 2 of 2001KC<sub>77</sub>. For the aforementioned 4 trajectories, the libration amplitudes range from 90° to 100°. By contrast, solution 1 of 2001KC<sub>77</sub> eventually yields circulation, while solution 3 leads to a close encounter with Neptune 0.512 Gyr into the simulation. For 1998WA<sub>31</sub>, all three solutions eventually end with a close encounter with Neptune, with solution 2 lasting the longest (0.882 Gyr). We conclude that among our three 5:2 resonant members, (38084) 1999HB<sub>12</sub> and possibly 2001KC<sub>77</sub> are likely to be long-term and therefore primordial residents of the 5:2 MMR. Note further that the accuracy of our orbital solution is highest for (38084) 1999HB<sub>12</sub> and lowest for 1998WA<sub>31</sub>; thus, it seems possible that with more astrometric measurements, all 3 objects will be found to stably occupy the 5:2 MMR over Gyr-long timescales.

Orbital elements for our three 5:2 resonant KBOs are provided in Table 1.

### 2.3. Observed Member of the 1:1 MMR

The evolution of the resonant argument,  $\phi_{1:1}$ , for object 2001QR<sub>322</sub> is displayed in Figure 5. Only the integration of the best-fit solution is shown; orbit solutions 2 and 3 yield nearly identical results. All three sets of initial conditions yield tadpole-type libration about Neptune’s L4 point for at least 1 Gyr. The libration center is  $\langle\phi_{1:1}\rangle \approx 64^\circ.5$ , the libration amplitude is  $\Delta\phi_{1:1} \approx 24^\circ$ , and the libration period is  $T_l \approx 10^4$  yr.

We further explore error space by integrating 8 additional solutions that deviate from the nominal best-fit solution by  $2\sigma$ ,  $3\sigma$ ,  $4\sigma$ , and  $5\sigma$ , each for 3 Myr. In all cases tested, object 2001QR<sub>322</sub> librates in the 1:1 MMR. We regard our identification of 2001QR<sub>322</sub> as a Neptunian Trojan as extremely secure.

The trajectory of the Trojan in the Neptune-centric frame is showcased in Figure 6. A tadpole-like path whose center is shifted forward in longitude from Neptune’s L4 point is evident; the longitude shift of  $\sim 5^\circ$  is expected for finite amplitude librators (see, e.g., Murray & Dermott 1999, their Figure 3.11). The minimum distance of approach to Neptune over 3 Myr is approximately 20 AU.

Orbital elements for our Trojan are listed in Table 1. Note that the orbital elements of 2001QR<sub>322</sub> lie consistently within the region of 4-Gyr-long stability mapped by Nesvorný &

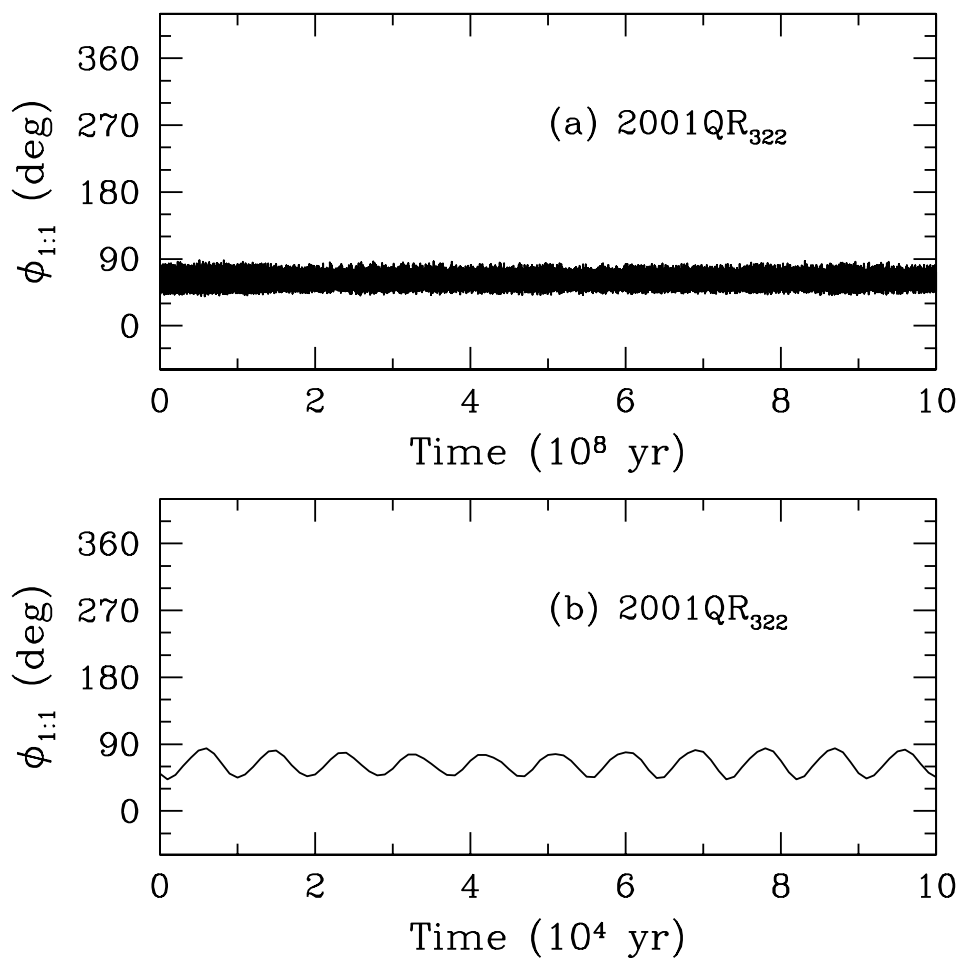


Fig. 5.— Evolution of the resonant argument,  $\phi_{1:1} = \lambda - \lambda_N$ , for our Neptunian Trojan, based on best-fit orbit solution 1. The object remains bound to the 1:1 resonance for at least 1 Gyr and betrays no sign of instability. Top and bottom panels display the same evolution with different time resolutions. Orbit solutions that deviate from the best-fit solution by as much as  $5\sigma$  also yield libration for at least 3 Myr (data not shown).

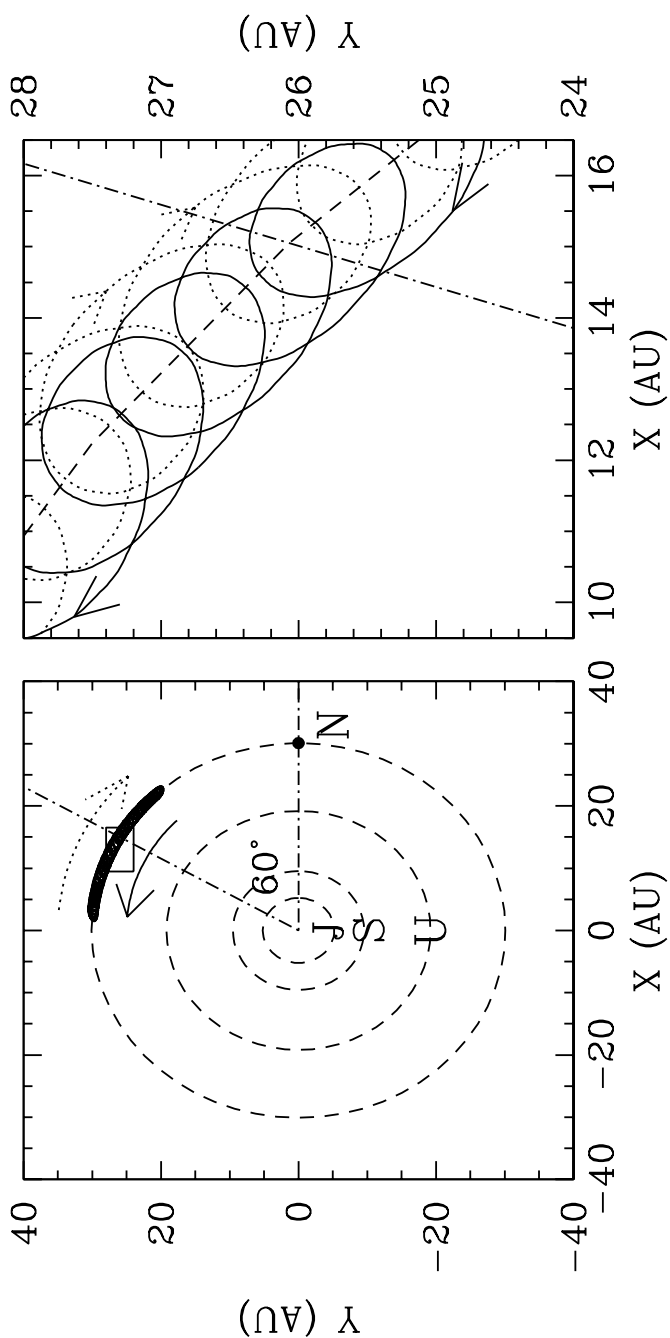


Fig. 6.— Trajectory of 2001QR<sub>322</sub>, our Neptunian Trojan, in a quasi-Neptune-centric frame. The left-hand panel displays a bird's-eye view of the outer solar system, with the giant planet orbits shown schematically. The dark tube of points lying on Neptune's orbit marks the computed path of the Trojan. The length of the vector from the origin to each point on the tube gives the instantaneous heliocentric distance of the object; the angle between this vector and the abscissa gives the instantaneous angle between the Sun-Trojan and Sun-Neptune vectors. The Trojan librates along Neptune's orbit as indicated by the solid and dotted curved arrows. Each libration takes about  $10^4$  yr to complete. The small inset rectangle is magnified in the right-hand panel to show the fast epicyclic motion. Each fast epicycle takes about 1 orbital period of Neptune, or about 200 yr, to complete.

Dones (2002); see their Figure 9c. Our object is a member of the low-inclination population of stable Neptunian Trojans; Nesvorný & Dones (2002) find surprisingly that Neptune Trojans having orbital inclinations as high as  $25^\circ$  are also stable. Note further that the libration amplitude of 2001QR<sub>322</sub> ( $24^\circ$ ) also lies consistently below the stability threshold of  $60\text{--}70^\circ$  established by Nesvorný & Dones (2002).

How many Neptunian Trojans might there be in all? Nesvorný & Dones (2002) provide three models of the sky density of Neptune Trojans that differ in the assumed distribution of orbital elements. We have combined their models (see their Figures 11, 13, and 14) with the distribution of our DES search fields to estimate that  $\sim 20$ ,  $\sim 60$ , and  $\sim 40$  Neptune Trojans having diameters and albedos comparable to those of 2001QR<sub>322</sub> exist in all, based on their models I, II, and III, respectively. The above numbers already include Trojans librating about Neptune’s L5 point, which we assume to have the same population as L4 librators. While it is impossible to differentiate between the models based only on the discovery of a single object, it is heartening to see that all 3 models give the same order-of-magnitude estimate for the total number of Neptune Trojans resembling 2001QR<sub>322</sub>.

### 3. Theoretical Implications of Resonance Occupation

Here we briefly explore theoretical implications of the observed occupation of the 5:2 and 1:1 Neptunian MMRs. We aim, in particular, to test the hypothesis that Neptune migrated outwards by several AU during the solar system’s past and, in so doing, sculpted the pattern of resonance occupation in the Kuiper belt (Fernandez & Ip 1984; Malhotra 1995; CJ). Sections 3.1 and 3.2 focus on the 5:2 MMR, while section 3.3 is devoted to the 1:1 MMR.

#### 3.1. Neptune’s Migration and the 5:2 MMR

Could KBOs in the 5:2 resonance have been trapped into that MMR as it swept across the Kuiper belt? We consider two scenarios, one in which Neptune migrates into a sea of initially dynamically cold test particles, and another in which the planet migrates into a sea of initially dynamically hot particles.

### 3.1.1. Cold Initial Conditions

For objects on initially low-eccentricity orbits, the probability of capture into the 5:2, third-order resonance is prohibitively small compared to the probability of capture into low-order resonances such as the 2:1 and 3:2. Neither the simulations performed by Malhotra et al. (2000), nor those by CJ report any object caught into the 5:2 resonance among the  $\sim 100$  test particles over which that resonance swept. We have executed another migration simulation, following those of CJ, that is tailored to gauge the capture efficiency of the 5:2 resonance for objects on initially nearly circular, low-inclination orbits. The simulation parameters are identical to those in CJ’s model I, except that the initial semi-major axes of the 400 test particles range from 43.55 AU (= 1 AU greater than the initial location of the 5:2 resonance) to 54.44 AU (= 1 AU less than the final location of the 5:2 resonance). Thus, all such objects are potentially swept into the migrating 5:2 resonance. Their initial eccentricities and inclinations are randomly and uniformly distributed between 0.00 and 0.05, and between 0.00 and 0.025 rad, respectively. Arguments of periastron ( $\omega$ ), longitudes of ascending nodes ( $\Omega$ ), and mean anomalies ( $M$ ) are uniformly and randomly sampled between 0 and  $2\pi$ . The semi-major axis of each giant planet evolves with time,  $t$ , according to

$$a(t) = a_f - (a_f - a_i) \exp(-t/\tau), \quad (1)$$

where we fix the migration timescale,  $\tau$ , to be  $10^7$  yr. We adopt values for the initial and final semi-major axes,  $(a_i, a_f)$ , for each of the planets as follows (in AUs): Jupiter (5.40, 5.20), Saturn (8.78, 9.58), Uranus (16.2, 19.2), and Neptune (23.1, 30.1). We employ the symplectic integrator, SyMBA (Duncan, Levison, & Lee 1998), as kindly supplied to us by E. Thommes. We adopt a timestep of 0.6 yr. For more details, the reader is referred to CJ.

Note that our simulations prescribe the migration to be smooth. If the planetesimals that scattered off Neptune and drove its migration were sufficiently massive, our idealization would be invalid. We estimate that our approximation is valid if most of the mass of the planetesimal disk were contained in bodies having radii less than  $\sim 40$  km. The derivation of our crude estimate is contained in the Appendix. The actual sizes of ancient planetesimals scattering off Neptune are, of course, unknown, though Kenyon (2002) calculates in his accretion simulations that  $\sim 90\%$  of the solid mass at heliocentric distances of 40–50 AU in the primordial solar system may be contained in 0.1–10 km-sized objects.

Figure 7 demonstrates that capture into the 5:2 resonance, even when Neptune takes as long as a few  $\times 10^7$  yr to migrate outwards by several AU, is improbable; only 1 out of 400 objects librates in the 5:2 resonance at the end of the simulation. By contrast, the 2:1 resonance boasts 90 captured objects. The predicted population ratio between the 5:2 and 2:1

resonances is not easily reconciled with the observations as depicted in Figure 3. Accounting for the observational bias in favor of finding 2:1 members over 5:2 members due to the fact that the 5:2 resonance is more distant than the 2:1 would only accentuate the disagreement. When both the effects of greater distance and differential longitudinal clustering of resonant KBOs are accounted for, we estimate that bias correction factors of  $\sim 3$  in favor of finding 2:1 members result (see CJ for a discussion of how these bias corrections are estimated). Even if the difference between the predicted 1-to-90 ratio vs. the observed 3-to-1 ratio were to be attributed to extremely strong and positive radial gradients in the primordial surface density of planetesimals (an unnatural prospect in itself), resonant excitation by the 5:2 MMR of initially cold orbits results in eccentricities and inclinations that are generally much too low compared with the observations.

Finally, we note that when non-DES and DES datasets are combined, the number of securely identified 2:1 resonant KBOs increases to 6. Blithely using this number, which is affected by observational biases from non-DES surveys that we have not quantified, still yields a ratio (3-to-6) that is hard to reconcile with the predicted ratio (1-to-90). The 6 2:1 resonant objects are (20161) 1996TR<sub>66</sub>, (26308) 1998SM<sub>165</sub>, 1997SZ<sub>10</sub>, 1999RB<sub>216</sub>, 2000JG<sub>81</sub>, and 2000QL<sub>251</sub>. Membership of 1997SZ<sub>10</sub> in the 2:1 resonance, and suspicion of membership of (20161) 1996TR<sub>66</sub>, were previously reported by Nesvorný & Roig (2001).

### 3.1.2. Hot Initial Conditions

Figure 8 displays the width of the 5:2 resonance in  $a$ - $e$  space. Since the resonance widens considerably at  $e \gtrsim 0.2$ , it is worth considering whether the capture efficiency increases with increasing initial eccentricity. Hot initial conditions prior to Neptune’s planetesimal-induced migration would be expected under the scenario of Thommes, Duncan, & Levison (1999, 2002). In their scenario, proto-Neptune and proto-Uranus are scattered by the other, nascent giant planets to heliocentric distances beyond 30 AU and heat the primordial Kuiper belt by gravitational scattering. That the Kuiper belt has been disturbed by more than the (hypothesized) slow sweeping of Neptune’s MMRs is evidenced by KBOs’ large orbital inclinations (Brown 2001; CJ).

We repeat the migration simulation of §3.1.1 but with initial eccentricities and inclinations of test particles uniformly and randomly distributed between 0 and 0.3, and between 0 and 0.15 rad, respectively. The result is summarized in Figure 9. Of 400 particles potentially caught by the sweeping 5:2 MMR, 20 are captured and have their eccentricities amplified to final values of 0.2–0.5. We have verified that these 20 objects represent adiabatic capture events and not violent scatterings; their semi-major axes increase smoothly over the duration

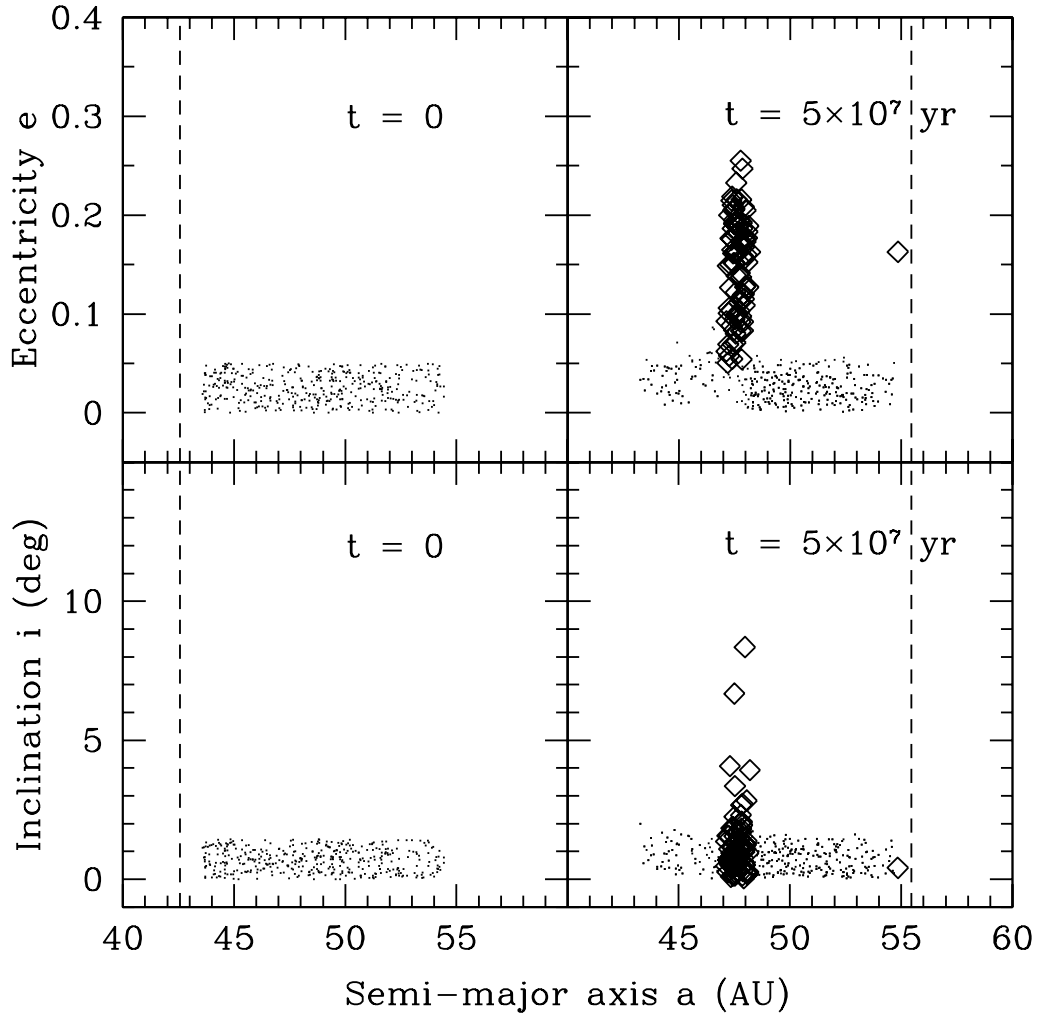


Fig. 7.— Results of a migration simulation designed to gauge the capture efficiency of the 5:2 resonance. Left-hand panels display cold initial conditions of 400 test particles prior to sweeping by the 5:2 resonance, whose nominal location is indicated by the dashed line. Right-hand panels display the aftermath of resonance sweeping, where open diamonds denote resonantly librating particles. Only 1 particle is caught by the 5:2 MMR; its eccentricity is pumped to 0.16 and its inclination is relatively unaltered. By contrast, 90 particles are swept into the 2:1 resonance at  $a \approx 47.8$  AU. The ratio of 1-to-90 is difficult to reconcile with the observed 3-to-1 ratio showcased in Figure 3; accounting for the bias introduced by the fact that the 5:2 MMR is more distant than the 2:1 would only worsen the disagreement. Moreover, the predicted final  $e$  and  $i$  of our simulated 5:2 resonant object are much lower than observed values.



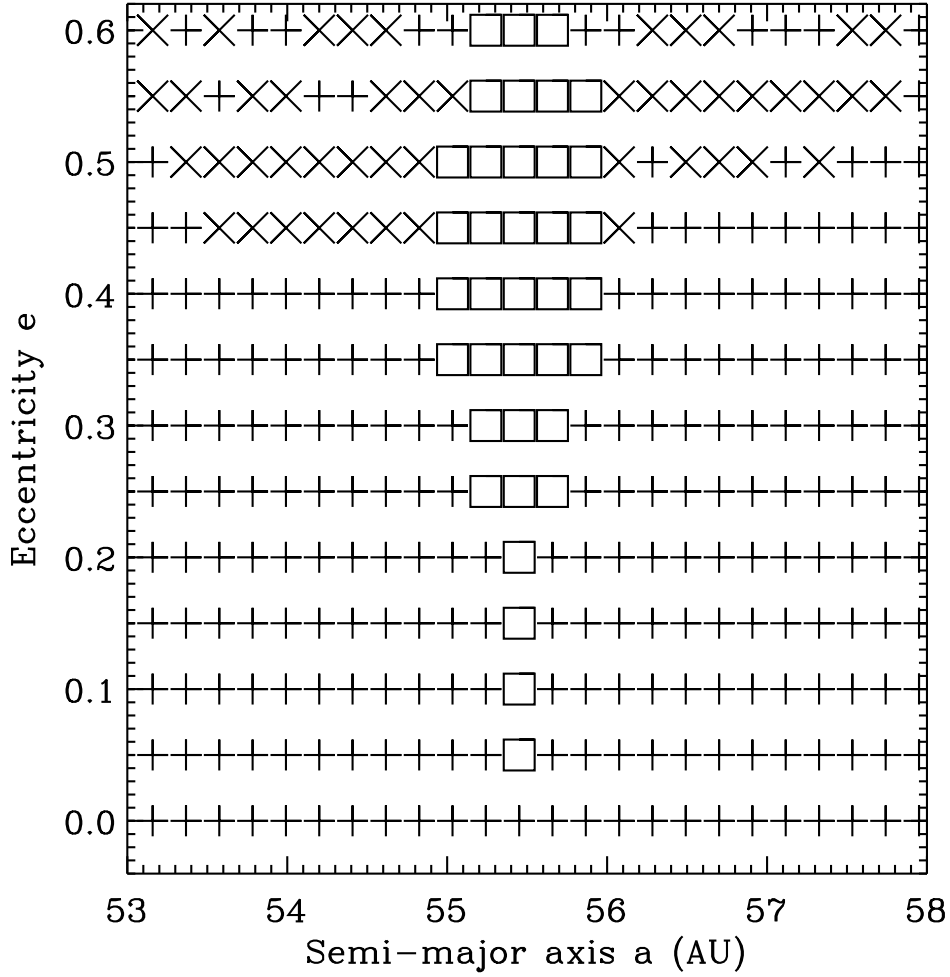


Fig. 8.— Estimated width of the 5:2 MMR, derived by numerical integration of the circular, planar, restricted 3-body model for the Sun/Neptune/KBO system. At each point on the above grid in  $a$ - $e$  space, a test particle’s trajectory is integrated in the gravitational fields of the Sun and Neptune for  $3 \times 10^5$  yr using a timestep of 0.6 yr. Test particles share the same initial  $i = 0$ ,  $\Omega = 0$ ,  $\omega = \pi/2$ , and  $M = 0$ . Initial elements of Neptune are given by  $a_N = 30.1$  AU,  $e_N = i_N = \Omega_N = \omega_N = M_N = 0$ . Thus, each particle’s initial  $\phi_{5:2} = \pi$ . Plus signs (“+”) denote particles for which  $\phi_{5:2}$  circulates; crosses (“x”) denote particles that encounter the Hill sphere of Neptune; and open squares denote particles that librate in the 5:2 MMR. The resonant width is greatest,  $\Delta a \approx 0.8$  AU, at  $e \gtrsim 0.2$ . Our 3-body model is used only to generate this figure and for no other figure in this paper.

of the simulation from values of as low as 45 AU to the final resonant value of 55.4 AU.

In addition, 5 objects are adiabatically swept into the 3:1 resonance whose final location lies at  $a \approx 62$  AU.

Are the predicted libration amplitudes consistent with those observed? The answer is yes; libration amplitudes of our 3 observed KBOs range from  $90^\circ$  to  $140^\circ$ , while those of our 20 simulated 5:2 resonant particles range from  $16^\circ$  to  $145^\circ$ , with 6 particles having amplitudes in the observed range.

While the capture efficiencies of high-order MMRs such as the 5:2 and 3:1 resonances magnify with increasing initial eccentricity, those of low-order MMRs such as the 3:2 and 2:1 resonances decrease. In the simulation just described, 29 objects are caught in the 2:1 resonance—a factor of 3 decline over the case with cold initial conditions. We have verified that these 29 objects are adiabatically captured by the sweeping 2:1 resonance and are not scattered into it by close encounters with one of the giant planets. These captured particles originated on low eccentricity orbits,  $e \lesssim 0.1$ .

Taken at face value, one problem with the simulation depicted in Figure 9 is that it predicts a large proportion of non-resonant particles having semi-major axes between 50 AU and 55 AU that, to date, are not observed. The problem of the “Kuiper Cliff”—a sudden decrease in the surface density of planetesimals outside 50 AU—has been discussed extensively in the literature (see, e.g., Jewitt, Luu, & Trujillo 1998; Gladman et al. 1998; Chiang & Brown 1999; Allen, Bernstein, & Malhotra 2001; Trujillo & Brown 2001). We regard the statistical significance of the observed edge of the belt as still marginal at best (see Allen et al. 2001). But even apart from possible observational selection biases, there are a number of factors that would help to improve the agreement between Figure 9 and observation. First, a fraction of the simulated non-resonant objects between  $a = 50$  AU and 55 AU have large eccentricities and are not phase-protected from Neptune, so that they are unlikely to survive in their current orbits for the age of the solar system. Second, if the “Kuiper Cliff” is real, we may impose an edge to our distribution at  $a = 50$  AU prior to resonance sweeping that would obviously reduce the number of objects in this region after resonance sweeping. The number of objects caught in the 5:2 MMR would be reduced by  $\sim 50\%$  compared to that shown in Figure 9. The resultant population ratio between the 5:2 and 2:1 MMRs of  $\sim 10$ -to- $29$  would still be reconcilable with the observations if we include the 5 other non-DES 2:1 objects listed in §3.1.1.

In summary, slow resonance sweeping over a primordial Kuiper belt that comprises both pre-heated orbits having  $i, e \gtrsim 0.2$  and cold orbits having  $e \lesssim 0.1$  is able to populate the 2:1 and 5:2 MMRs with efficiencies that do not seem irreconcilable with the observations.

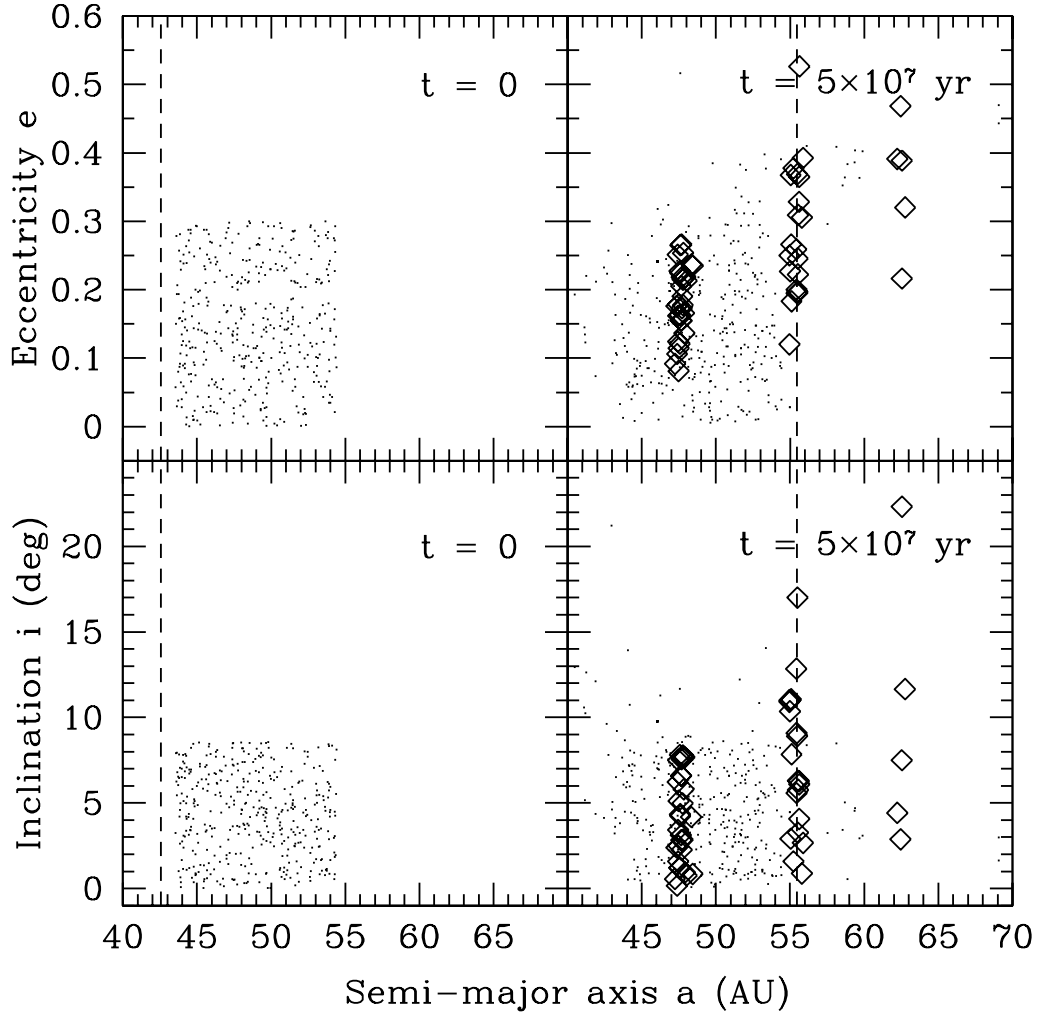


Fig. 9.— Results of a migration simulation designed to gauge the capture efficiency of the 5:2 resonance under hot initial conditions. Left-hand panels display hot initial conditions of 400 test particles prior to sweeping by the 5:2 resonance, whose nominal location is indicated by the dashed line. Right-hand panels display the aftermath of resonance sweeping. Open diamonds denote librating particles in the 2:1, 5:2, and 3:1 MMRs. Twenty particles are adiabatically swept into the 5:2 MMR and have their eccentricities and inclinations excited above their initial values. Twenty-nine particles are swept into the 2:1 resonance at  $a \approx 47.8$  AU. The libration amplitudes of the simulated 5:2 resonant KBOs range from  $16^\circ$  to  $145^\circ$ , with 6 particles having amplitudes in the range between  $90^\circ$  and  $140^\circ$  (data not shown). The relative efficiencies of capture into the 2:1 and 5:2 MMRs, the predicted libration characteristics of 5:2 resonant particles, and the large final eccentricities and inclinations of resonant particles can all be reconciled with the observations, in contrast to the case using only cold initial conditions.

The models can be tuned to match the observations by adjusting the initial eccentricity, inclination, and semi-major axis distributions of belt particles prior to the migration phase. We have not undertaken such tuning here; our main conclusion is that capture into the 5:2 MMR is made substantially more efficient, and generates 5:2 resonant orbits similar to those observed, by pre-heating the belt prior to resonance sweeping. Of course, our finding does not address the question of what was responsible for this pre-heating.

### 3.2. Direct Scattering into the 5:2 MMR

Is it possible that KBOs in the 5:2 MMR may not have been captured via resonance sweeping, but were rather gravitationally scattered into that resonance by close encounters with one or more massive objects? In  $a$ - $e$ - $i$  space, the proximity of our 5:2 resonant KBOs to orbits traditionally described as “scattered” suggests direct scattering by Neptune as a population mechanism. To test this hypothesis, we integrate the trajectories of 400 test particles on initially low-eccentricity, low-inclination orbits in the vicinity of Neptune. The test particles’ semi-major axes, eccentricities, and inclinations range between 31.7 AU and 35.7 AU (2–7 Neptunian Hill radii from Neptune’s semi-major axis), 0.00 and 0.02, and 0.00 and 0.01 rad, respectively. The other orbital angles are uniformly and randomly distributed between 0 and  $2\pi$ . The duration of the integration is  $5 \times 10^7$  yr. No migration is imposed on any of the planets, whose initial positions and velocities are taken from Cohen, Hubbard, & Oesterwinter (1973). We again employ the symplectic integrator, SyMBA; this integrator handles close encounters with better accuracy than does `swift_rmvs3`. We adopt a timestep in the absence of close encounters of 0.6 yr.

Figure 10 summarizes the results of this simulation of direct scattering into MMRs. Of 400 test particles, 0, 1, 2, and 1 particles are scattered into the 3:1, 5:2, 2:1, and 3:2 MMRs. These resonant KBOs have substantial eccentricities, between 0.19 and 0.45. Thus, the existence of resonant KBOs having high eccentricities, taken at face value, does not necessarily imply capture and adiabatic excitation by migratory resonances. The relative capture efficiencies between the 3:1, 5:2, 2:1, and 3:2 MMRs in our direct scattering simulation do not appear irreconcilable with the observations, given the small number statistics (both observationally and theoretically), observational biases (CJ), and uncertainties regarding actual initial conditions.

Direct scattering by Neptune, however, predicts libration amplitudes that are generally larger than those observed. For our (4) simulated resonant particles inhabiting the 5:2, 2:1, and 3:2 MMRs, libration amplitudes all exceed  $160^\circ$ . This is to be compared, for example, with the libration amplitudes exhibited by our three observed 5:2 resonant KBOs,

which range between  $90^\circ$  and  $140^\circ$  (see Figure 4). While we cannot rule out the possibility that 1998WA<sub>31</sub> represents such a directly scattered, dynamically young object based on its unstable behavior on timescales of Myrs to Gyrs (see §2.2), the small libration amplitudes of (38084) 1999HB<sub>12</sub> and 2001KC<sub>77</sub> do not match those predicted by the scattering simulation. (And as noted in §2.2, it remains possible that future improvements in the accuracy of the trajectory of 1998WA<sub>31</sub> may cause it to join its more stable brethren.)

The problem of excessive libration amplitudes was reported in a similar context by Levison & Stern (1995), who investigated ways to excite Pluto’s orbit to its present high eccentricity and inclination using only gravitational interactions with the giant planets in their current orbits. Possible resolutions to this difficulty include invoking physical collisions with and/or gravitational scatterings off primordial KBOs (Levison & Stern 1995). The disagreement between predicted and observed libration characteristics seems particularly severe for the 2:1 resonant objects. In our direct scattering simulation, the two particles scattered into the 2:1 MMR librate with large amplitude about  $\langle\phi_{2:1}\rangle = 180^\circ$ . This conflicts with the observed small libration amplitudes about  $\langle\phi_{2:1}\rangle \approx 75^\circ$ : the single confirmed Twotino in our survey librates with small libration amplitude ( $50^\circ$ ) about  $\langle\phi_{2:1}\rangle \approx 88^\circ$ , while four secure non-DES Twotinos are characterized by  $\langle\phi_{2:1}\rangle \approx 70^\circ, 67^\circ, 74^\circ$ , and  $83^\circ$  (see CJ). Only one secure non-DES Twotino (2000JG<sub>81</sub>) resembles a simulated particle, librating about  $\langle\phi_{2:1}\rangle = 180^\circ$  with an amplitude of  $160^\circ$ . Note that we interpret the observed asymmetrically librating Twotinos to be primordial residents, since they resemble the stable particles simulated by Nesvorny & Roig (2001; see their section 3.4).

Is it possible that our simulation contains too few particles to fully explore phase space, and that we have been unlucky in the outcome of libration profiles? We do not believe so. Objects barely bound to MMRs are to be expected from the direct scattering hypothesis, because for Neptune to heat the orbit of a test particle significantly, the distance of closest approach must be small, within several Hill radii of Neptune. During the (brief) close encounter, a particle’s velocity is radically altered; but because the particle’s position during the encounter is relatively unchanged, subsequent close approaches between particle and planet will occur at similarly small distances. Large libration amplitude is synonymous with small distance of closest approach; thus, close encounters with Neptune alone are expected to yield only tenuously bound resonant particles whose resonant locks are easily broken.

### 3.3. Neptune’s Migration and the 1:1 MMR

Gomes (1998) explores, via numerical simulations similar to those presented here, the ability of a migratory Neptune to *retain* (as opposed to capture) a Trojan population. A

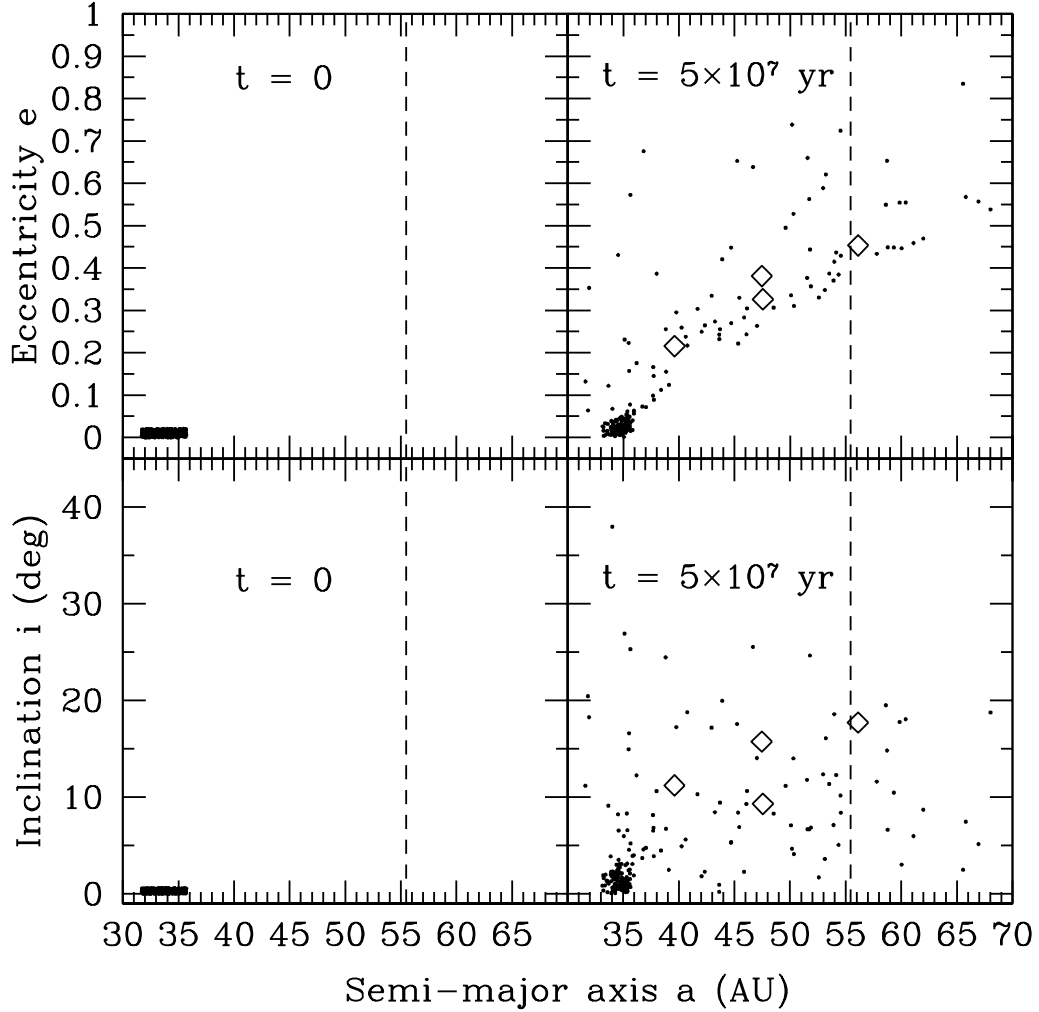


Fig. 10.— Results of a direct scattering simulation in which no migration is imposed on any of the planets. Left-hand panels display cold initial conditions for 400 test particles situated between 2 and 7 Neptunian Hill radii from Neptune. Right-hand panels display conditions after 50 Myr. One, two, and one particles, represented by open diamonds, are scattered directly into the 5:2, 2:1, and 3:2 MMRs, respectively. The eccentricities, inclinations, and relative numbers of these particles appear consistent with the observations. However, the predicted and observed libration characteristics disagree. The four simulated resonant particles have libration amplitudes between  $160^\circ$  and  $175^\circ$  (data not shown in this figure), too large compared to the moderate amplitudes observed.

variety of migration histories for the giant planets are tested; between 20% and 82% of his hypothetical Neptunian Trojans remain bound to the 1:1 MMR throughout the migration phase. He concludes that unless the migration history of the giant planets was such as to engender divergent resonance crossings and excitation of planetary eccentricities to values of  $\sim 0.1$ —a history that would, *prima facie*, conflict with the small orbital eccentricities currently exhibited by Uranus and Neptune—a Neptunian Trojan population might be expected to exist today. This finding is strongly reinforced by Nesvorný & Dones (2002), who find for their hypothesized Neptune Trojans that about 50% of them survive for 4 Gyr in a post-migration solar system.

Distinct from the retainment efficiency of the 1:1 MMR is the efficiency with which a migrating Neptune captures objects into the 1:1 MMR; this capture efficiency has not been reported in the literature. To remedy this deficiency, we execute a migration simulation similar to the one described in §3.1.1, except that the initial semi-major axes of the 400 test particles are distributed between 24.1 AU (= 1 AU greater than the initial location of the 1:1 MMR) and 29.1 AU (= 1 AU less than the final location of the 1:1 MMR). Only cold initial conditions (initial  $0 \leq e \leq 0.05$ ,  $0 \leq i \leq 0.025$ ) are employed; hot initial conditions would conflict with the observed low  $e$  and low  $i$  of 2001QR<sub>322</sub>. This is because, as described in greater detail below, migration is not expected to significantly alter the eccentricities and inclinations of Trojans. Results of the migration simulation are displayed in Figure 11. Of 400 particles potentially swept into the 1:1 MMR, no particle is captured. The overwhelming fate of the particles is to be scattered to larger semi-major axes, eccentricities, and inclinations. The low capture efficiency of  $\lesssim 0.0025$  suggests that Neptunian Trojans do not owe their existence to Neptune’s migration. Our conclusion is subject to the caveat that we have not modelled a possible stochastic component to Neptune’s migration; see §3.1.1 and the Appendix.

Capture scenarios that invoke frictional drag from solar nebular gas, and damping of libration amplitudes via gaseous envelope accretion by the host planet, are characterized by healthy capture efficiencies for Jupiter’s Trojans (Marzari & Scholl 1998; Peale 1993), but are expected to be less efficient for Neptune’s Trojans. The decrease in efficiency arises because Neptune’s hydrogen/helium component amounts to only  $\sim 5\text{--}20\%$  of Neptune’s total mass, while Jupiter’s hydrogen/helium component comprises  $\sim 90\%$  of that planet’s mass (Lissauer 1995). We also note that frictional drag was likely to have been ineffective if 2001QR<sub>322</sub> possessed its current diameter (estimated 130–230 km, assuming a 12–4% albedo) at the time of capture; 2001QR<sub>322</sub> must have grown from the collisional agglomeration of smaller bodies that did feel gas drag (Peale 1993).<sup>8</sup>

---

<sup>8</sup>We note in passing that Neptune’s irregular satellite, Triton, might be thought of as inhabiting a 1:1

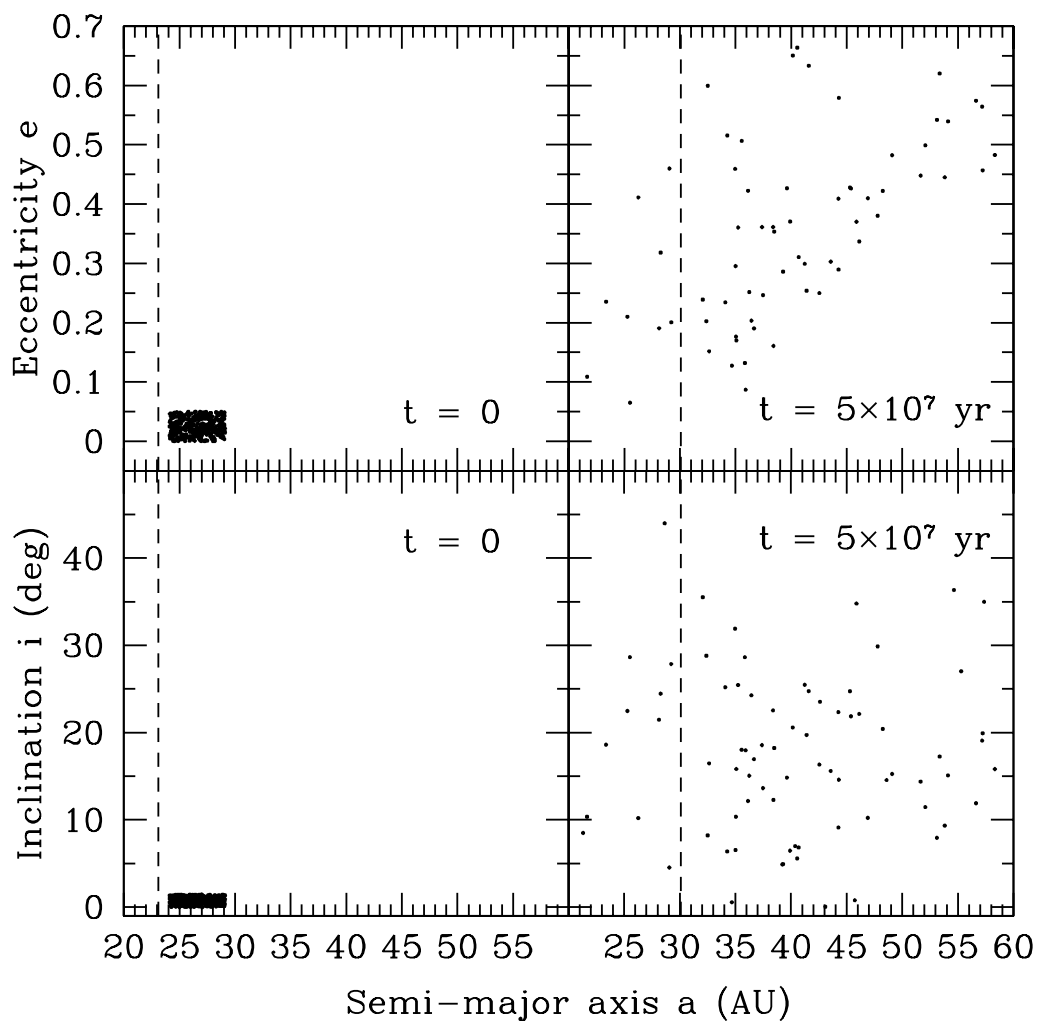


Fig. 11.— Results of a migration simulation designed to gauge the capture efficiency of the 1:1 resonance. Left-hand panels display cold initial conditions of 400 test particles prior to sweeping by the 1:1 resonance, whose nominal location is indicated by the dashed line. Right-hand panels display the aftermath of resonance sweeping. No particle is captured into a Trojan-type orbit. Particles instead suffer close encounters with Neptune and are scattered onto highly eccentric and inclined orbits.



We now justify our earlier assertion that hot initial conditions prior to resonance capture into the 1:1 resonance are inappropriate for 2001QR<sub>322</sub>. Unlike the case of exterior resonances, outward migration causes the eccentricities and inclinations of Trojans to decline. This behavior can be seen from the adiabatic invariant,  $C_{pq}$ , associated with a MMR for which the ratio of mean orbital periods is  $p:(p+q)$  ( $p$  and  $q$  are integers and  $q < 0$  for exterior resonances):

$$C_{pq} = \sqrt{M_{\odot}a} [(p+q) - p\sqrt{1-e^2} \cos i] \quad (2)$$

$$\approx \frac{\sqrt{M_{\odot}a}}{2} (e^2 + i^2). \quad (3)$$

(see, e.g., Yu & Tremaine 2001). For the last equality, we have taken  $p = 1$ ,  $q = 0$ , and  $e, i \ll 1$ . Then as  $a$  increases,  $e^2 + i^2$  must decrease. Fleming & Hamilton (2000) find in numerical simulations that, indeed, both eccentricity and inclination decrease as the semi-major axis increases, in quantitative agreement with the adiabatic invariant. The effect is extremely weak. If we take  $i^2$  to be always comparable to  $e^2$  (as we can for the current orbit of 2001QR<sub>322</sub>), then  $(e_f/e_i) \approx (i_f/i_i) \approx (a_i/a_f)^{1/4}$ . Migration scenarios adopt, for Neptune,  $0.7 \lesssim a_i/a_f \leq 1$ ; then the eccentricities and inclinations of its Trojans decline by at most 10% due to outward migration.

Perhaps the most natural time for Neptune to accrue its Trojans is during its assembly from planetesimals. For mass accretion timescales that are long compared to the Trojan libration period, a 30-fold increase in the mass of the host planet reduces the libration amplitudes of Trojans by factors of 2–3 (Fleming & Hamilton 2000).

#### 4. Summary and Discussion

We have presented, as part of our ongoing Deep Ecliptic Survey, the most complete picture of mean-motion resonance occupation in the Kuiper belt to date (Figure 3). We have discovered members of the 5:2, 2:1, 7:4, 3:2, 4:3, and 1:1 resonances. These KBOs represent secure identifications in the sense that (1) their  $1\sigma$  fractional uncertainties in semi-major axis lie between 3% and 0.003%, and (2) numerical integrations of orbit solutions distributed over the  $1\sigma$  confidence surface of possible fitted orbits consistently yield resonant arguments that librate for at least 3 Myr. In the special cases of the 1:1 and 5:2 resonances,

---

resonance with Neptune and might have been captured from an initially heliocentric orbit by colliding with an ancient regular satellite of Neptune (Goldreich et al. 1989).

we have checked by explicit numerical orbit integrations that orbit solutions distributed over  $5\sigma$  confidence surfaces also yield libration for at least 3 Myr, and that orbit solutions distributed over  $1\sigma$  confidence surfaces yield libration for up to 1 Gyr for our 1:1 resonant object and for a subset of our 5:2 resonant objects.

Object 2001QR<sub>322</sub>, the first discovered Neptunian Trojan, librates about the leading Lagrange (L4) point of Neptune. Numerical integrations of its trajectory that account for the presence of the four giant planets reveal that libration persists for at least 1 Gyr. Furthermore, the orbital elements of 2001QR<sub>322</sub> and its small libration amplitude of  $24^\circ$  are consistent with the properties of Neptunian Trojans that are stable for 4 Gyr, as described by, e.g., Nesvorny & Dones (2002). It seems unlikely that the Trojan was captured into the 1:1 MMR purely by dint of Neptune’s hypothesized migration; as Neptune encroaches upon an object, the latter is sooner scattered onto a highly eccentric and inclined orbit than caught into co-orbital resonance. More probably, Neptunian Trojans pre-date the migration phase and owe their existence to the same process that presumably gave rise to the Jovian Trojans: trapping of planetesimals into libration about the L4/L5 points of an accreting protoplanetary core (Marzari & Scholl 1998; Fleming & Hamilton 2000). Subsequent outward radial migration by Neptune due to the scattering of planetesimals causes  $\sim 20$ – $82\%$  of Neptunian Trojans to escape the resonance (Gomes 1998), and decreases the eccentricities and inclinations of the remaining bound fraction by modest amounts,  $\sim 10\%$  at most. Taken together, the long-term stability of 2001QR<sub>322</sub> (this paper; Nesvorny & Dones 2002) and its relative insensitivity to dramatic changes in Neptune’s orbit lead us to regard Neptunian Trojans as dynamically pristine compared to the rest of the Kuiper belt. The 1:1 MMR acts as a shelter against close encounters and dynamical excitation by resonance sweeping. It is possible that the Trojan has always remained confined to heliocentric distances of 20–30 AU.

For an assumed albedo of 12–4%, our Neptune Trojan is 130–230 km in diameter. When our DES search fields are overlaid on model-dependent predictions of the sky density of Neptunian Trojans constructed by Nesvorny & Dones (2002), we estimate that between  $\sim 20$  and  $\sim 60$  Neptune Trojans resembling 2001QR<sub>322</sub> librate about Neptune’s L4 and L5 points. For comparison, about  $\sim 10$  Jovian Trojans exist having diameters between 100 and 200 km (Davis et al. 2003).

Our Deep Ecliptic Survey has uncovered 3 members of the 5:2 MMR. Among all resonant KBOs, these objects possess the highest orbital eccentricities and substantial orbital inclinations. Their orbits cannot be a consequence of the standard model of Neptune’s migration; they cannot have originated from low- $e$ , low- $i$  orbits that underwent resonant capture and adiabatic excitation by a migratory Neptune. The probability of resonant capture into the 5:2 MMR under cold initial conditions is too small compared with the probabilities of

capture into the 2:1 and 3:2 MMRs; the standard model predicts a population ratio of  $\sim 0.01$  between the 5:2 and 2:1 MMRs that is not easily reconciled with the observed ratio of  $\sim 3$ . Moreover, the orbital eccentricities and inclinations of 5:2 resonant objects that are predicted by the standard model are too low compared with their observed values.

The inability of the 5:2 MMR to capture objects on low eccentricity orbits is reflected in the vanishingly small width of the resonance at  $e = 0$ . By contrast, we have found by numerical simulations akin to those that produced Figure 8 that the 2:1 and 3:2 MMRs both *widen* as  $e$  decreases from 0.05 to 0. Note that estimates by Malhotra (1996) of resonant widths do not extend to  $e < 0.05$ . Murray & Dermott (1999; see their Figure 8.7) discuss this qualitative difference between the low-eccentricity behavior of first-order interior MMRs and that of higher-order interior MMRs. We reserve a more detailed theoretical exploration of the dynamics and capture efficiencies of exterior MMRs to a future study.

The simplest channel for populating the 5:2 MMR with objects like those that we have observed involves adiabatically slow sweeping of that MMR over a *pre-heated* Kuiper belt, i.e., one containing a significant proportion of initially high- $e \gtrsim 0.2$ , high- $i \gtrsim 0.2$  orbits prior to the migration phase. Capture efficiencies increase at large  $e$  for the 5:2 resonance, a reflection of the greater width of this resonance at large  $e$  and its vanishingly small width at small  $e$ . The libration amplitudes predicted by resonance sweeping over a pre-heated belt are moderate, between  $16^\circ$  and  $145^\circ$ , and accord well with those observed.

Direct scattering of objects into the 5:2 and other resonances via close encounters with Neptune can also generate the large eccentricities and inclinations that are observed, but generally fails to reproduce the observed libration properties. Direct scattering yields objects that are barely bound to MMRs; large libration amplitudes exceeding  $160^\circ$  are predicted for the 5:2, 2:1, and 3:2 MMRs, in conflict with the observations. Additional mechanisms—gravitational interactions and/or physical collisions with bodies other than Neptune—would need to be invoked to dampen libration amplitudes. Levison & Stern (1995) elaborate on a series of events that can dampen the libration amplitude of Pluto in the 3:2 resonance; analogous events would need to be invoked to dampen the libration amplitudes of members of other MMRs. These mechanisms require the ancient Kuiper belt to be orders of magnitude more populous than it is today, a prospect that by itself does not appear unreasonable, given the requirements of planet formation models (Kenyon 2002), and ongoing dynamical (Holman & Wisdom 1993; Duncan, Levison, & Budd 1995) and collisional erosion of the belt.

Nonetheless, we feel that Occam’s razor, and the physical plausibility and seeming inevitability of planetary migration driven by planetesimal scattering (Fernandez & Ip 1984; Hahn & Malhotra 1999), would seem to disfavor resonance population mechanisms that

do not invoke migration. Perhaps the principal objection to this mechanism lies in the possibility that Neptune’s migration was insufficiently smooth to resonantly capture objects; we discuss quantitatively this possibility in the Appendix. Chiang & Jordan (2002) offer a more objective test of the migration hypothesis; for sufficiently fast migration rates, the number of 2:1 resonant KBOs having libration centers  $\langle\phi_{2:1}\rangle \approx 270^\circ$  should exceed those having  $\langle\phi_{2:1}\rangle \approx 90^\circ$  by factors of  $\sim 3$ . An asymmetry in libration center populations translates directly into an asymmetry in the sky density of Twotinos about the Sun-Neptune line. By contrast, if the 2:1 resonance were populated by direct scattering, the libration centers would presumably be equally populated. At present, the number (6) of known Twotinos is too small to permit the drawing of firm conclusions.

In summary, it is most straightforward to reproduce the observed pattern of resonance occupation in the Kuiper belt by presupposing both initially cold orbits (to populate resonances such as the 3:2 and 2:1 MMRs) and initially hot orbits (to populate resonances such as the 5:2 MMR) prior to Neptune’s migration.

What might have heated the primordial Kuiper belt prior to resonance sweeping? Models of planetesimal formation predict eccentricities and inclinations of less than  $\sim 0.05$  (see, e.g., Kenyon & Luu 1999; Lissauer 1993; Kokubo & Ida 1992), values below what are required to capture KBOs into the 5:2 resonance with the relative efficiencies observed. Thommes, Duncan, & Levison (1999, 2002) propose that the  $\sim 10 M_\oplus$  embryonic cores of Neptune and Uranus were scattered into the ancient belt and heated KBOs by dynamical friction. A possible problem with this scenario is that Neptune’s orbital history may be too violent to generate a significant Trojan population.

By contrast, we believe there exists another pre-heating mechanism that is more natural: scattering of KBOs to large  $e$  and large  $i$  by Neptune as that planet migrated outwards (Gomes 2002). The formation of a primitive scattered disk that is later swept over by mean-motion resonances seems a natural consequence of planetary migration driven by planetesimal scattering. What requires further elucidation is how the perihelia of the scattered objects are raised so as to avoid further scatterings by Neptune.

We are indebted to Dr. Jana Pittichova for donating her telescope time to secure astrometric observations of our Neptune Trojan that helped to solidify its dynamical identity. EIC acknowledges support from National Science Foundation Planetary Astronomy Grant AST-0205892, Hubble Space Telescope Theory Grant HST-AR-09514.01-A, and a Faculty Research Grant awarded by the University of California at Berkeley. MWB, RLM, and LHW are supported in part by NASA grants NAG5-8990 and NAG5-11058. Research by JLE and SDK is supported, in part, by NASA grant NAG5-10444. DET is supported by grants

from the American Astronomical Society and the Space Telescope Science Institute. KJM is supported by NASA grant NAG5-4495. We thank Kelly Clancy and Mark Krumholz for assistance, and David Nesvorny for a thoughtful referee’s report that significantly improved this paper. The NOAO observing facilities used in the Deep Ecliptic Survey are supported by the National Science Foundation.

### A. Breakdown of Smooth Migration

Here we crudely estimate the critical sizes of Neptune-encountering planetesimals above which our assumption of smooth migration would be invalid. We imagine that at each instant during Neptune’s migration, Neptune’s annulus of influence— $r_H \sim (m_N/3m_\odot)^{1/3}a_N$  in extent, where  $m_N$  and  $m_\odot$  are the mass of Neptune and of the Sun, respectively, and  $a_N$  is the semi-major axis of Neptune—contains  $N$  planetesimals each having  $\Delta m$  mass. A typical Poisson fluctuation in the number of planetesimals is  $\sqrt{N}$ . It is this random fluctuation that generates a change of random sign in Neptune’s semi-major axis, by an amount of order  $\delta a \sim \sqrt{N}(\Delta m/m_N)a_N$  after all the planetesimals within the annulus of influence are scattered away. The duration of encounter between each planetesimal and Neptune is of order Neptune’s orbital period,  $P_N$ . Then the magnitude of the random component of Neptune’s migration rate is of order  $\delta a/P_N$ .

For the migration to be smooth,

$$\delta a/P_N < \dot{a}_{mean}, \tag{A1}$$

where  $\dot{a}_{mean}$  is the mean (smooth) migration rate that arises from the mean difference in Neptune-encountering fluxes having high specific angular momentum and fluxes having low specific angular momentum. In our simulations,  $\dot{a}_{mean} = \Delta a_N \exp(-t/\tau)/\tau$ , where  $\Delta a_N = 7$  AU and  $\tau = 10^7$  yr.

We estimate the surface mass density of planetesimals within the annulus of influence to be the surface mass density of planetesimals throughout the disk. Hahn & Malhotra (1999) find in their numerical simulations of planetary migration (using effective particle sizes too large to engender smooth migration) that  $m_{disk} \sim 50M_\oplus$  of material must be interspersed between  $a = 10$  AU and  $a_{disk} = 50$  AU to drive Neptune’s orbit outward by  $\Delta a_N \approx 7$  AU. Then our order-of-magnitude estimate for the surface mass density everywhere is  $N\Delta m/\pi r_s^2 \sim m_{disk}/\pi a_{disk}^2$ . We solve this equation for  $N$ , and insert into condition (A1) to find

$$\frac{\Delta m}{m_N} < \left(\frac{a_{disk}}{a_N}\right)^2 \left(\frac{\Delta a_N}{r_H}\right)^2 \left(\frac{P_N}{\tau}\right)^2 \left(\frac{m_N}{m_{disk}}\right) \exp(-2t/\tau). \quad (\text{A2})$$

For  $m_N = 17M_{\oplus}$ ,  $a_N = 25$  AU,  $r_H = 0.6$  AU,  $P_N = 130$  yr,  $t = \tau = 10^7$  yr, and other parameters as listed above, we find that  $\Delta m/m_N < 4 \times 10^{-9}$  for the migration to be smooth. Spheres of density  $2 \text{ g cm}^{-3}$  having radii less than 40 km would suffice. If Neptune’s migration instead occurred over timescales of  $\tau = 3 \times 10^6$  yr, the critical radius grows to 80 km. Kenyon (2002) calculates that 90% of the mass of the primordial Kuiper belt was contained in bodies having radii of 0.1–10 km at heliocentric distances of 40–50 AU. It is not clear, however, how these accretion calculations should be modified at distances of 20–30 AU where Neptune resided. An inopportune encounter between Neptune and a single massive planetesimal might have caused the former to lose whatever retinue of resonant objects it had accumulated previously by smooth migration.

## REFERENCES

- Allen, R.L., Bernstein, G.M., & Malhotra, R. 2001, *ApJ*, 549, L241
- Bernstein, G., & Khushalani, B. 2000, *AJ*, 120, 3323
- Brown, M.E. 2001, *AJ*, 121, 2804
- Chiang, E.I., & Brown, M.E. 1999, *AJ*, 118, 1411
- Chiang, E.I., & Jordan, A.B. 2002, *AJ*, 124, 3430 (CJ)
- Cohen, C., Hubbard, E., & Oesterwinter, C. 1973, *Elements of the outer planets for one million years*, U.S. Naval Observatory Nautical Almanac, 22, 1
- Davis, D.R., Durda, D.D., Marzari, F., Bagatin, A.C., & Gil-Hutton, R. 2003, in *Asteroids III*, eds. W.F. Bottke, A. Cellino, P. Paolicchi, and R.P. Binzel (Tucson: University of Arizona Press), 545 (preprint)
- Duncan, M.J., Levison, H.F., & Budd, S.M. 1995, *AJ*, 110, 3073
- Duncan, M.J., Levison, H.F., & Lee, M.-H. 1998, *AJ*, 116, 2067
- Elliot, J.L., et al. 2003, in preparation
- Fernandez, J.A., & Ip, W. H. 1984, *Icarus*, 58, 109
- Fleming, H.J., & Hamilton, D.P. 2000, *Icarus*, 148, 479
- Gladman, B., et al. 1998, *AJ*, 116, 2042
- Goldreich, P., Murray, N., Longaretti, P.Y., & Banfield, D. 1989, *Science*, 245, 500

- Gomes, R. 1998, *AJ*, 116, 2590
- Gomes, R. 2002, DPS Meeting #34, poster #17.05
- Hahn, J.M., & Malhotra, R. 1999, *AJ*, 117, 304
- Holman, M., & Wisdom, J. 1993, *AJ*, 105, 1987
- Holman, M. 1995, The Distribution of Mass in the Kuiper Belt, Proceedings of the Twenty-Seventh Symposium on Celestial Mechanics, eds. Hiroshi Kinoshita and Hiroshi Nakai
- Jewitt, D.C., & Luu, J.X. 2000, in *Protostars and Planets IV*, eds. V. Mannings, A.P. Boss, and S.S. Russell (Tucson: University of Arizona Press), 1201
- Jewitt, D., Luu, J., & Trujillo, C. 1998, *AJ*, 115, 2125
- Kenyon, S., & Luu, J. 1999, *AJ*, 118, 1101
- Kenyon, S. 2002, *PASP*, 114, 265
- Kokubo, E., & Ida, S. 1992, *PASJ*, 44, 601
- Levison, H.F., & Duncan, M.J. 1994, *Icarus*, 108, 18 (<http://k2.boulder.swri.edu/~hal/swift.html>)
- Levison, H.F., & Stern, S.A. 1995, *Icarus*, 116, 315
- Lissauer, J.J. 1993, *ARA&A*, 31, 129
- Malhotra, R. 1995, *AJ*, 110, 420
- Malhotra, R., Duncan, M.J., & Levison, H.F. 2000, in *Protostars and Planets IV*, eds. V. Mannings, A.P. Boss, and S.S. Russell (Tucson: University of Arizona Press), 1231
- Marzari, F., & Scholl, H. 1998, *Icarus*, 131, 41
- Millis, R., et al. 2002, *AJ*, 123, 2083
- Murray, C.D., & Dermott, S.F. 1999, *Solar System Dynamics* (New York: Cambridge University Press)
- Nesvorny, D., & Dones, L. 2002, *Icarus*, 160, 271
- Nesvorny, D., & Roig, F. 2001, *Icarus*, 150, 104
- Peale, S.J. 1993, *Icarus*, 106, 308
- Thommes, E.W., Duncan, M.J., & Levison, H.F. 1999, *Nature*, 402, 635
- Thommes, E.W., Duncan, M.J., & Levison, H.F. 2002, 123, 2862
- Trujillo, C.A., & Brown, M.E. 2001, *ApJ*, 554, L95
- Wisdom, J., & Holman, M. 1991, *AJ*, 102, 1528

Yu, Q., & Tremaine, S. 2001, AJ, 121, 1736



Table 1. Orbital Elements<sup>a</sup> of DES 5:2 and 1:1 Resonant KBOs

Name	Resonance	$a$ (AU)	$e$	$i$ (deg)	$\Omega$ (deg)	$\omega$ (deg)	$M$ (deg)
1998WA <sub>31</sub>	5:2	55.73	0.432	9.43	20.7	310.7	28.2
(38084) 1999HB <sub>12</sub>	5:2	55.10	0.409	13.17	166.5	66.7	343.1
2001KC <sub>77</sub>	5:2	54.67	0.352	12.9	57.8	181.8	358.4
2001QR <sub>322</sub>	1:1	30.39	0.028	1.32	151.6	236.2	327.3

<sup>a</sup>Osculating, heliocentric elements referred to the J2000 ecliptic plane, evaluated at epoch 2451545.0 JD. Elements shown here are best-fit values; for a discussion of uncertainties, see §2.1 and Elliot et al. (2003). The angles  $\Omega$ ,  $\omega$ , and  $M$  are the longitude of ascending node, the argument of perihelion, and the mean anomaly, respectively.

Table 2. Designations of DES and Non-DES Resonant KBOs

Resonance	Name
1:1	2001QR <sub>322</sub> *
5:4	1999CP <sub>133</sub>
4:3	1998UU <sub>43</sub> *, 2000CQ <sub>104</sub> *, (15836) 1995DA <sub>2</sub>
3:2	(28978) Ixion*, 1998UR <sub>43</sub> *, 1998US <sub>43</sub> *, 1998WS <sub>31</sub> *, 1998WU <sub>31</sub> *, 1998WV <sub>31</sub> *, 1998WW <sub>24</sub> *, 1998WZ <sub>31</sub> *, 2000CK <sub>105</sub> *, 2001KY <sub>76</sub> *, 2001KB <sub>77</sub> *, 2001KD <sub>77</sub> *, 2001KQ <sub>77</sub> *, 2001QF <sub>298</sub> *, 2001QG <sub>298</sub> *, 2001RU <sub>143</sub> *, 2001RX <sub>143</sub> *, (15788) 1993SB, (15789) 1993SC, (15810) 1994JR <sub>1</sub> , (15820) 1994TB, (15875) 1996TP <sub>66</sub> , (19299) 1996SZ <sub>4</sub> , (20108) 1995QZ <sub>9</sub> , (24952) 1997QJ <sub>4</sub> , (32929) 1995QY <sub>9</sub> , (33340) 1998VG <sub>44</sub> , (38628) 2000EB <sub>173</sub> , (47171) 1999TC <sub>36</sub> , (47932) 2000GN <sub>171</sub> , 1993RO, 1995HM <sub>5</sub> , 1996RR <sub>20</sub> , 1996TQ <sub>66</sub> , 1998HH <sub>151</sub> , 1998HK <sub>151</sub> , 1998HQ <sub>151</sub> , 1999CE <sub>119</sub> , 1999CM <sub>158</sub> , 1999TR <sub>11</sub> , 2000FV <sub>53</sub> , 2000GE <sub>147</sub> , 2001FL <sub>194</sub> , 2001VN <sub>71</sub> , 2001YJ <sub>140</sub> , 2002VE <sub>95</sub> , 2001FU <sub>172</sub>
5:3	(15809) 1994JS, 1999CX <sub>131</sub> , 2001XP <sub>254</sub>
7:4	2000OP <sub>67</sub> *, 2001KP <sub>77</sub> *, 1999KR <sub>18</sub> , 1999RH <sub>215</sub> , 2000FX <sub>53</sub> , 2000OY <sub>51</sub>
2:1	2000QL <sub>251</sub> *, (20161) 1996TR <sub>66</sub> , (26308) 1998SM <sub>165</sub> , 1997SZ <sub>10</sub> , 1999RB <sub>216</sub> , 2000JG <sub>81</sub>
7:3	1999CV <sub>118</sub>
5:2	(38084) 1999HB <sub>12</sub> *, 1998WA <sub>31</sub> *, 2001KC <sub>77</sub> *, (26375) 1999DE <sub>9</sub> , 2000FE <sub>8</sub> , 2000SR <sub>331</sub> , 2002TC <sub>302</sub>

<sup>a</sup>Objects discovered by DES are denoted by an asterisk.